LA-UR- 09-05306

Approved for public release; distribution is unlimited.

Title:	nanoMechanics at High P-T Conditions
Author(s):	Yusheng Zhao
Intended for:	IUCr and AIRAPT meetings

Los Alamos NATIONAL LABORATORY EST.1943

Form 836 (7/06)

Nano-Mechanics at High P-T conditions.

Deformation and Yield Strength of nano-Materials at High Pressures

High *P-T* Comparative Studies on Nano-/Micron- Crystallines and Molecular Inclusion Compounds — *Constitutive Property, Elastic Modulus, Bonding Structures, and Encapsulating Capability, etc.*

Yusheng Zhao

yzhao@lanl.gov

LANSCE - Lujan Center
Los Alamos National Laboratory

Outline:

High P-T tests on nano-grain's crystalline modeling
Pressure effects by molecular cages and frameworks

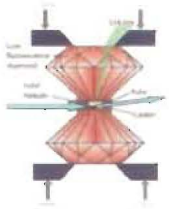

Diamond Anvil Cell

Six Anvil Compression

Cubic Anvil Cell Assembly

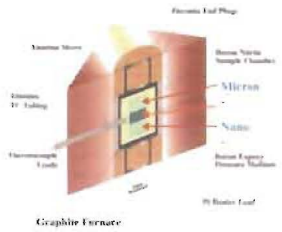

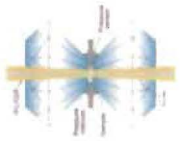

Techniques Applied:

Diffractions under High *P-T* Conditions *using* Synchrotron X-Ray & Time-of-Flight Neutron

Transparencies in diffraction optics

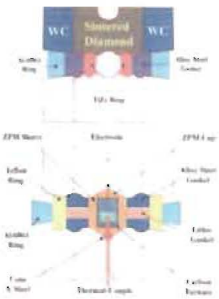

90° Bank

Toroidal Anvil Press

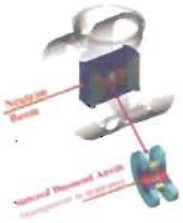

Macro- *vs* micro-

under pressures

Powder Compaction

(*micro-strain*)

Deviatoric Stress

(*macro-strain*)

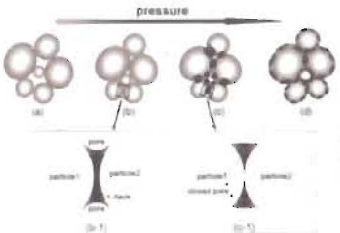

***grain-to-grain* contact stress concentration**

(a), relaxed lattice
(no stress applied on the "infinite" atomic lattices)

(b), macro-strains
(stress field applied to the overall sample)

(c), micro-strains
(stress concentration due to grain-to-grain contacts)

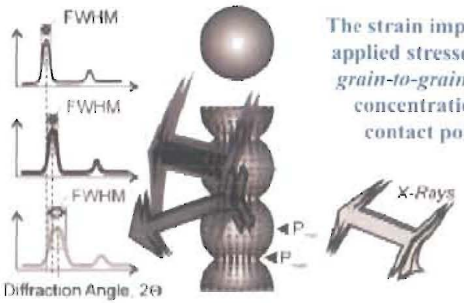

The strain imposed by applied stresses & by *grain-to-grain* stress concentration at contact points

nano-crystal

Uniform Core and Strained Surface

***Palosz* Model**

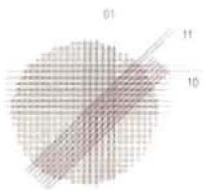

(a)

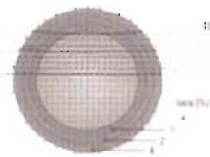

(b)

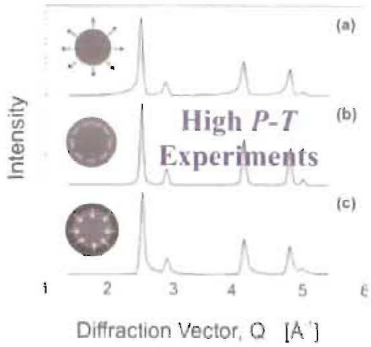

Lattice strain information as reflected in diffraction peak position and peak width

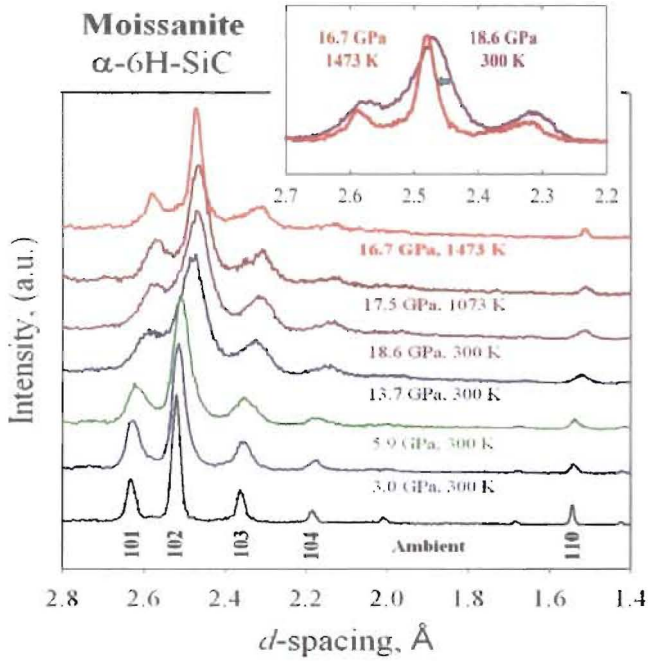

$$Int.(d) \propto exp\left[-\left(\frac{d-d_{hkl}}{s}\right)^2\right] \qquad s=\sqrt{d^2-\bar{d}^2}=\Delta d(FWHM)$$

Gaussian expression for the de-convoluted peak width

$$\Delta d^2_{obs.} = \Delta d^2_{ins.} + \Delta d^2_{size} + \Delta d^2_{\varepsilon}(P,T)$$

$$\varepsilon = \Delta d / d$$

$$\left\{ \Delta d^2_{obs.} - \Delta d^2_{ins.} \right\} = \Delta d^2_{size} + \varepsilon^2 \cdot d^2(P,T)$$

$$\varepsilon = \Delta d_{\varepsilon} / d = \sqrt{\Delta d^2_{obs.} - \Delta d^2_{ins.}} \Big/ d(P,T)$$

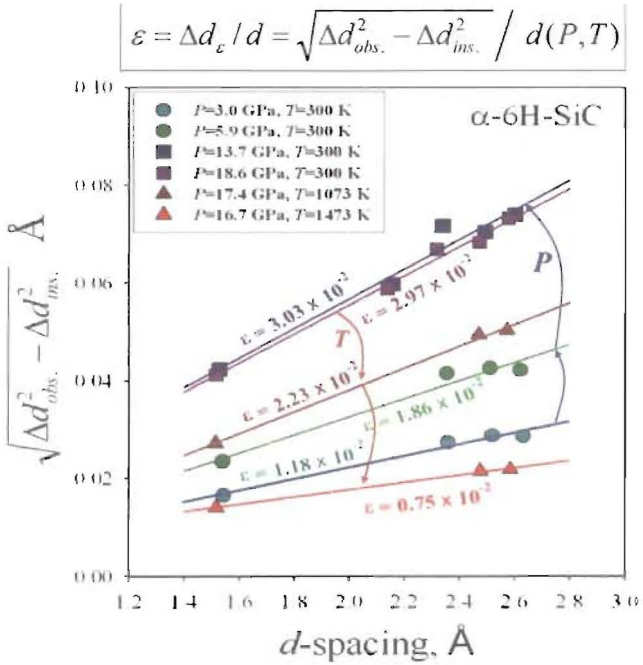

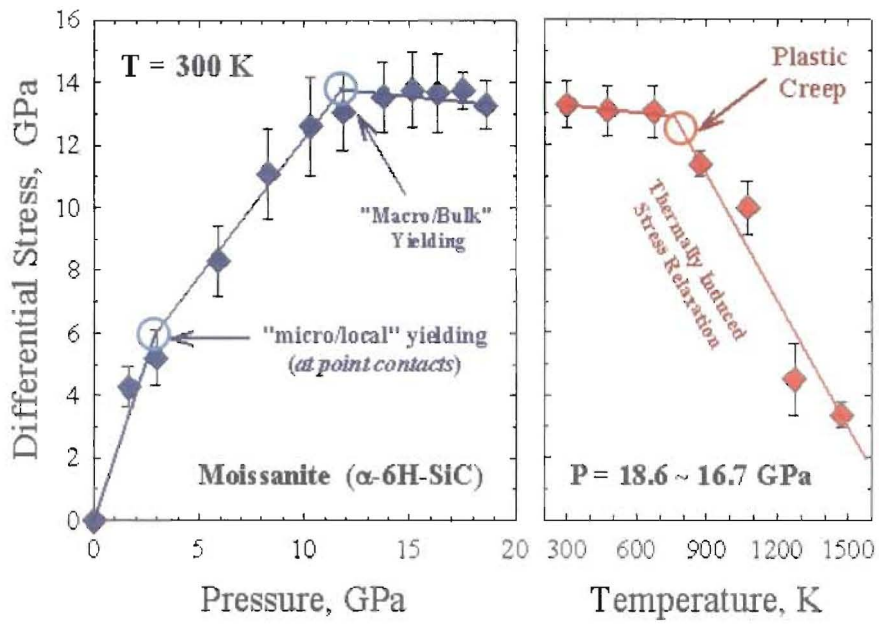

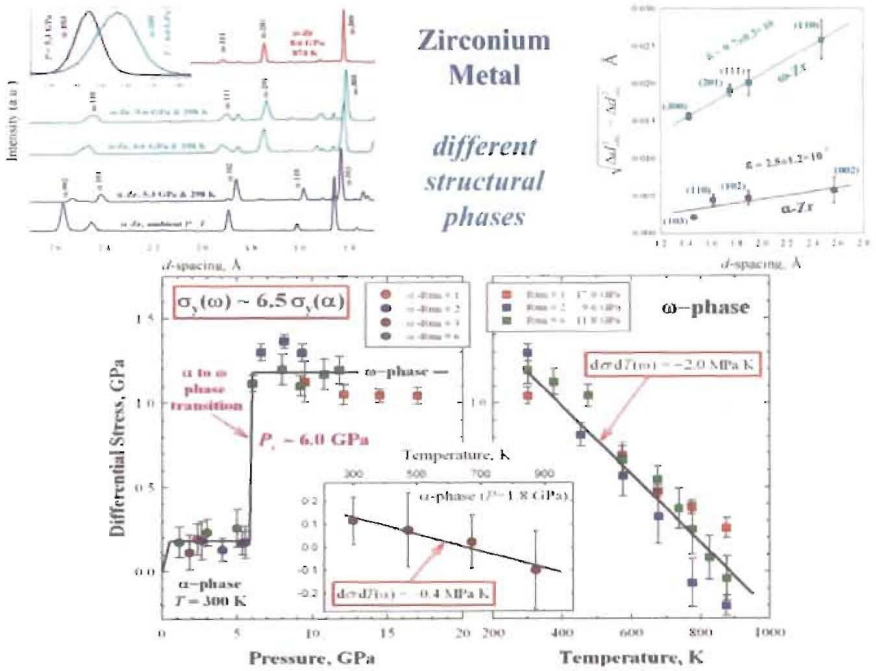

The Scherrer formula (Scherrer, 1918) describes grain size in diffraction:

$$L = k \cdot \lambda / \Delta(2\theta)_{size} \cos\theta$$

where k is the Scherrer constant and $\Delta(2\theta)_{size}$ is the FWHM in (2θ) at a constant wavelength λ, in angular dispersive mode. By differentiating Bragg's diffraction equation, $\lambda = 2d \cdot \sin\theta$, with respect to d and 2θ, respectively, it becomes:

$$\Delta(2\theta) = -2(\Delta d / d)\tan\theta$$

We substitute into the Gaussian expression for the de-convoluted peak width and normalize the formula to a general definition of overall strain $\Delta d/d$, thus have:

$$L = k \cdot d^2 / \Delta d_{size}(\mathrm{FWHM})$$

which is independent of detecting mode. We substitute into the Gaussian expression for the de-convoluted peak width and normalize the formula to a general definition of overall strain $\Delta d/d$, thus have:

$$\Delta d^2_{obs.}/d^2 = \left(\varepsilon^2 + \Delta d^2_{ins.}/d^2\right) + \left(\kappa/L\right)^2 \cdot d^2(P,T)$$

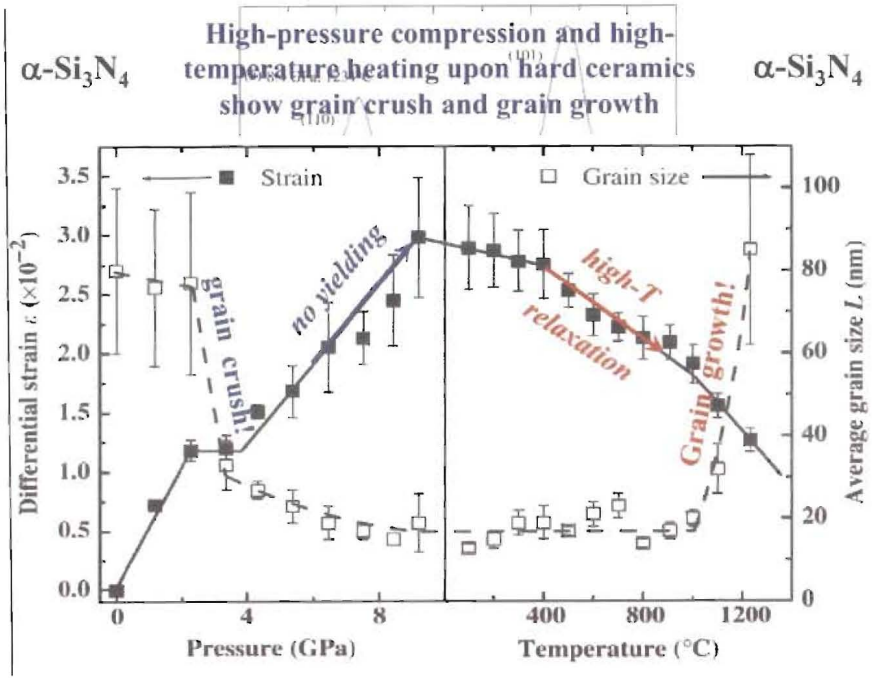

High *P-T* diffraction study of nano-/micron- nickel samples (*comparative!*)

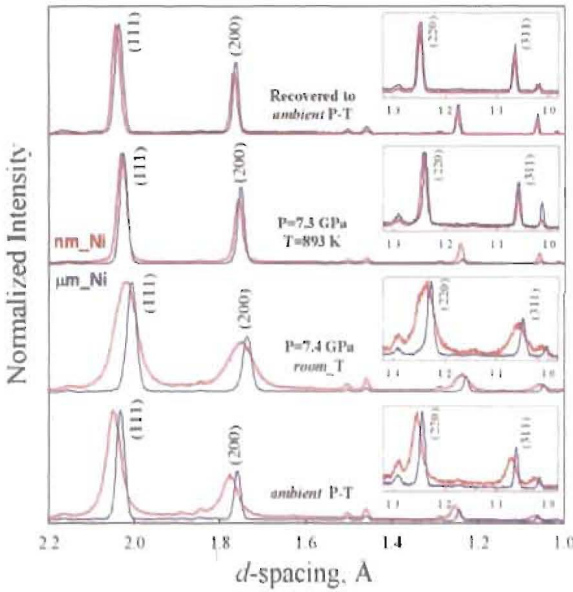

- Peak broadening → contact stresses at high pressures
- Peak sharpening → stress relaxation & grain growth
- Hi-T grain growth of nano Ni at T > 873 K
- FWHM (high-T) < FMHM (ambient)
- Peak shift in nano Ni: grain size reduction & impurity effect of Fe

Significant data scattering observed for the nano-Ni compared with the micron-Ni in the strain derivation *via* $\Delta d^2/d^2$ plot fit

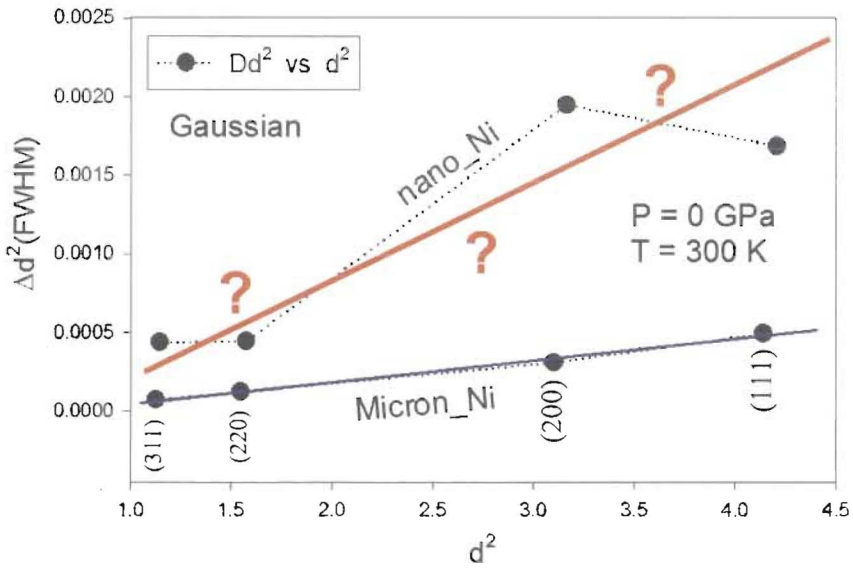

The data scattering of nano-Ni become even more sever at high-*P*

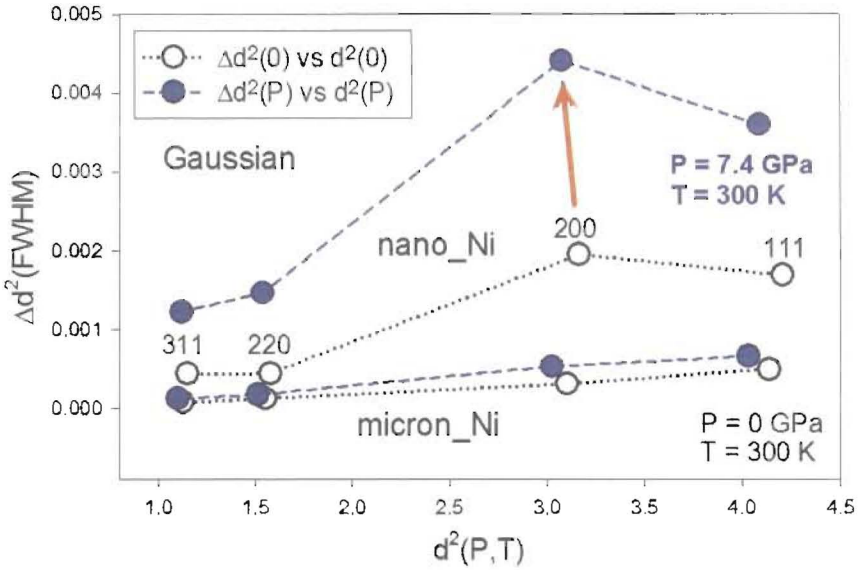

The diffraction elastic compliances S_1 and S_2 of the individual (hkl) planes for the nickel metal are derived using single crystal elastic constants. We further derive Young's modulus

$$E_{hkl} = 1 \Big/ \left(S_1 + \frac{1}{2} S_2 \right)$$ ***Diffraction Elastic Modulus***

hkl	S_1 (10^{-3}/GPa)	$\frac{1}{2}S_2$ (10^{-3}/GPa)	E_{hkl} (GPa)	E_{hkl}/E_{200}
(111)	-1.241	5.529	233.2	1.331
(200)	-1.956	7.663	175.2	1.000
(220)	-1.420	6.065	215.3	1.229
(311)	-1.619	6.663	198.3	1.132

By multiplying $DER^2 = (E_{hkl}/E_{200})^2$ to the observed raw data, we ***correct*** the strain differences on individual lattice planes. By choosing the most compliant planes, the (200) peaks, as reference we derive the upper bound for the apparent strain.

$$\Delta d^2_{obs.}/d^2 = \left(\varepsilon^2 + \Delta d^2_{ins.}/d^2\right) + (\kappa/L)^2 \cdot d^2(P,T)$$

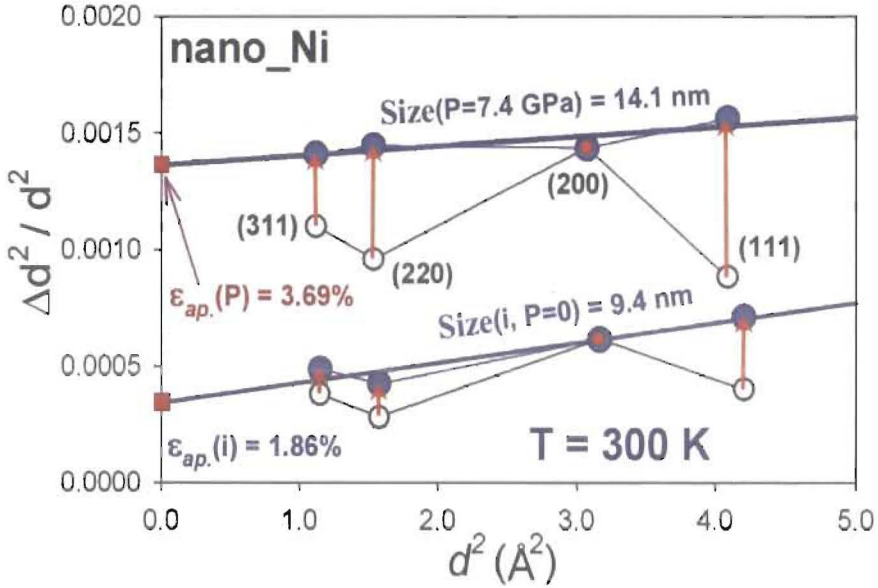

High *P-T* Constitutive Property of Nano-/Micron- Nickel Polycrystallines

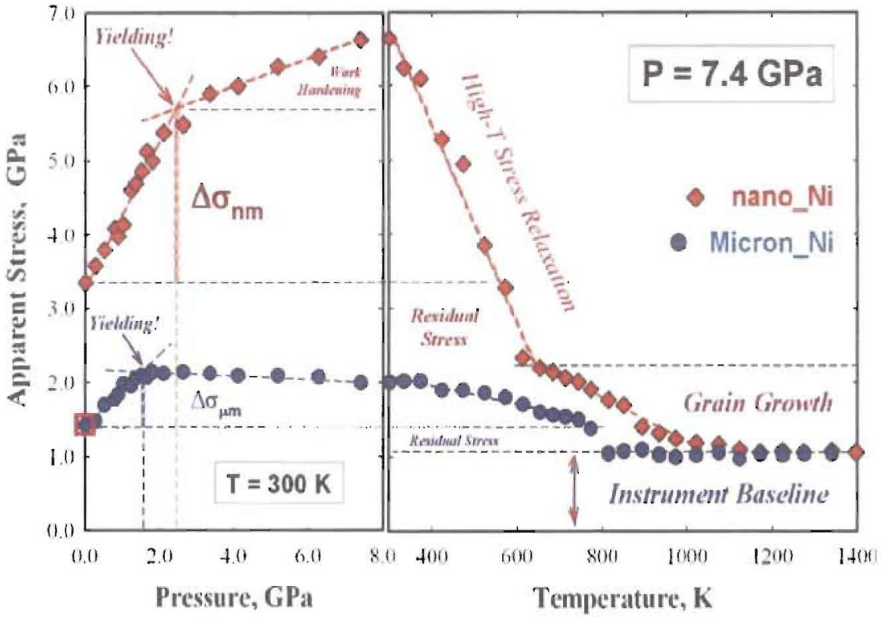

High-*T* Annealing and Grain Growth of Nano-Ni

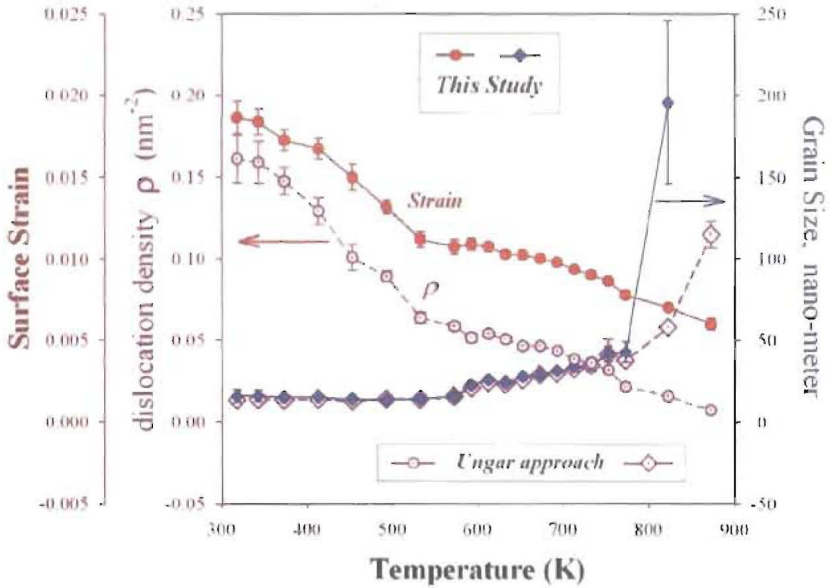

The Recoverability:

$$\textbf{Rec.} = [\bar{\varepsilon}(\max.P) - \bar{\varepsilon}(end)]/\bar{\varepsilon}(\max.P)$$

- Apparent strain: $E_{hkl} = \Delta d(\text{FWHM})/d$
- Lattice planes of different *hkl* strain at different levels
- **Two yield points in μm Ni: "micro/local" deformation "macro/bulk" deformation**
- Pronounced non-linear ductility and continuous work hardening in nano Ni
- **Significant difference in strain recoverability after unloading**

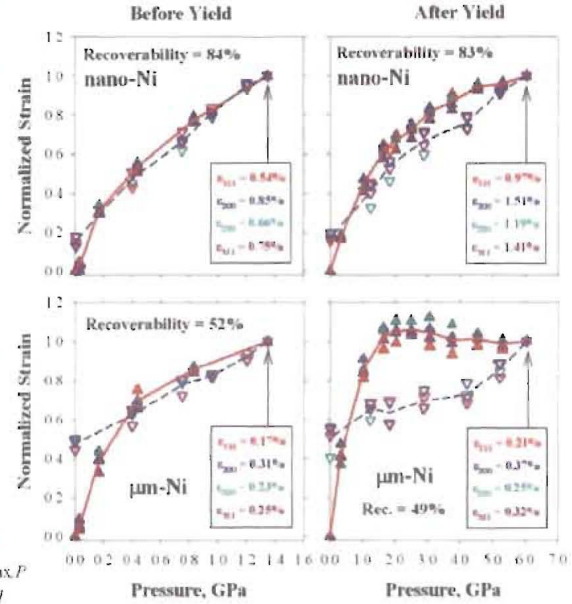

$$\varepsilon_{hkl}^{norm} = \left(\Delta d/d\right)_{hkl} \Big/ \left(\Delta d/d\right)_{hkl}^{\max.P}$$

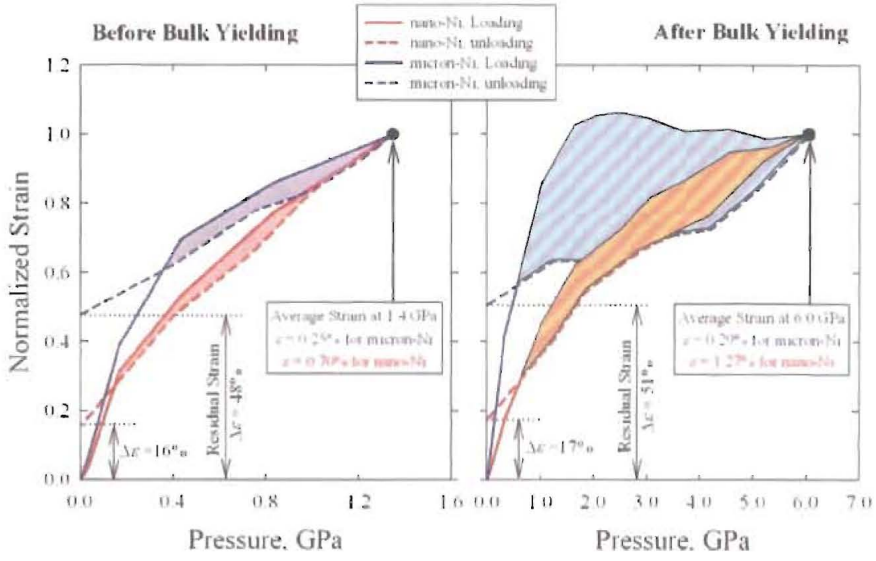

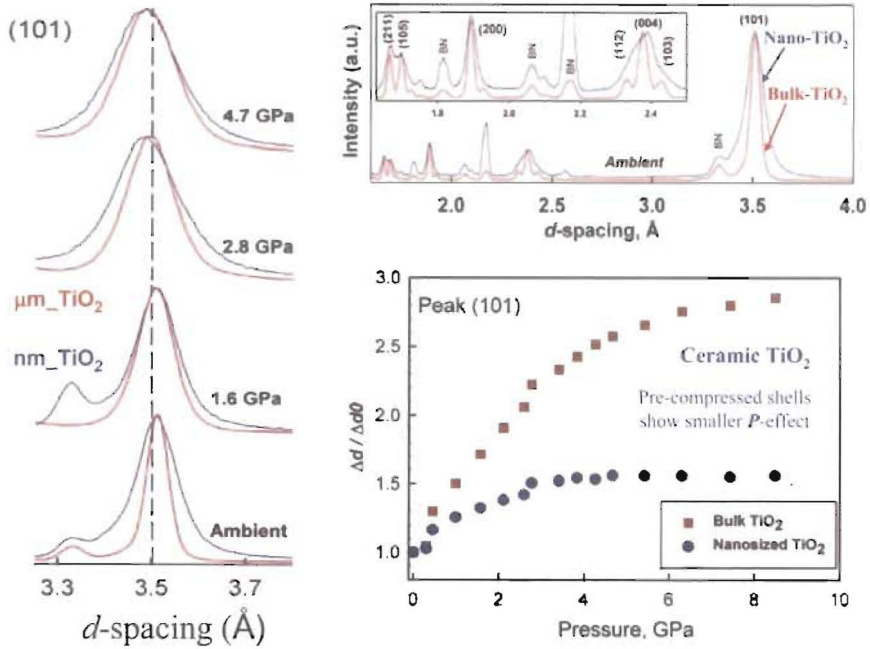

Nano-TiO_2 shows lower yield strength than micron-TiO_2

Similarity between nano-TiO_2 and micron-Ni in double yielding and work softening

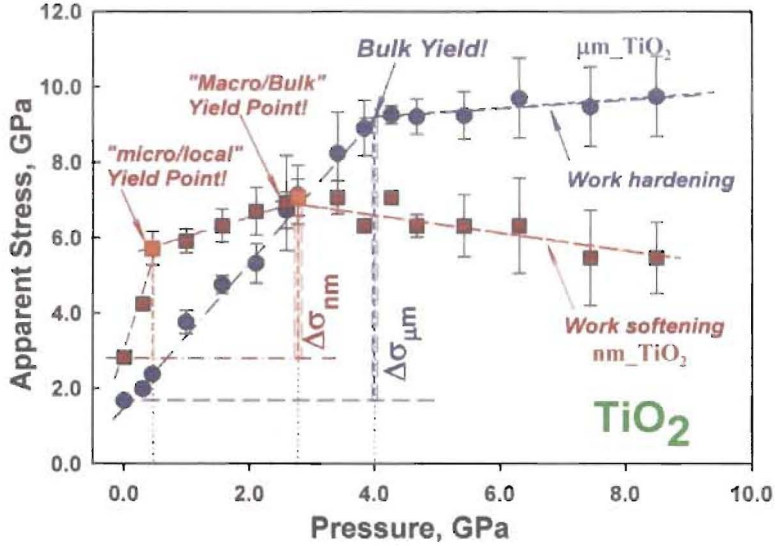

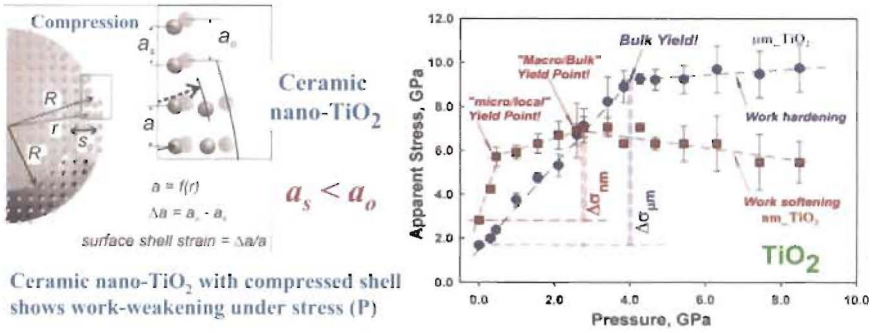

Ceramic nano-TiO_2 with compressed shell shows work-weakening under stress (P)

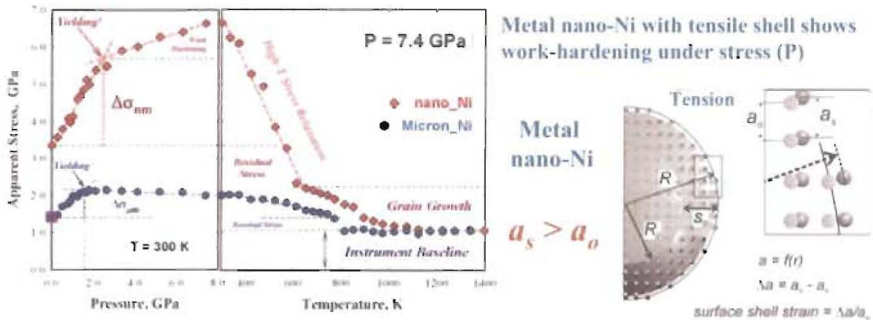

Metal nano-Ni with tensile shell shows work-hardening under stress (P)

Initial enhancement of bulk modulus observed for the nano-ceramics may result from the "pre-" **compressed** surface lattices in the **shell** volume of the nano- crystal grains;

The high pressure induced work-weakening/cold-welding type of grain growth ***fuse*** surface shell with bulk cores, correspondingly the elastic modulus reduces/approaches the bulk values at high-pressures after P_t.

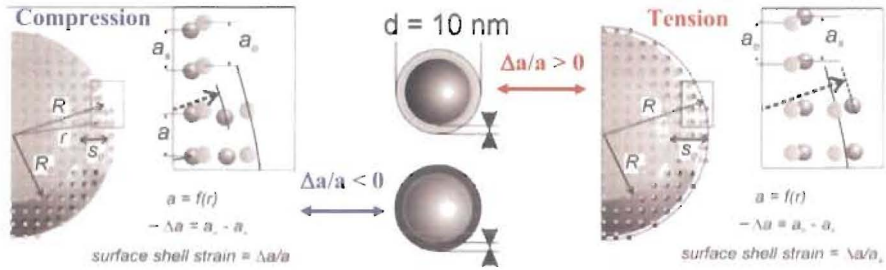

Initial reduction of bulk modulus observed for the nano-metals may result from the "pre-" **expanded** surface lattices in the **shell** volume of the nano- crystal grains;

The high pressure induced work-hardening after the bulk yield reflects continuous densification of the surface shell while the bulk core also experience compression

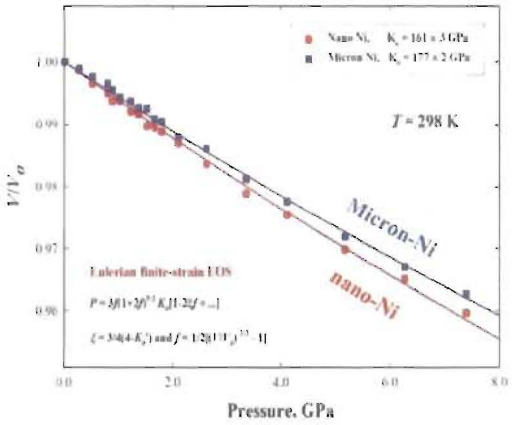

Overall, the nano-Ni is ~10 percent more compressible than micron-Ni

Tensile surface shell of the nano-Ni metal is *17-18%* more compressible than its gain core interior

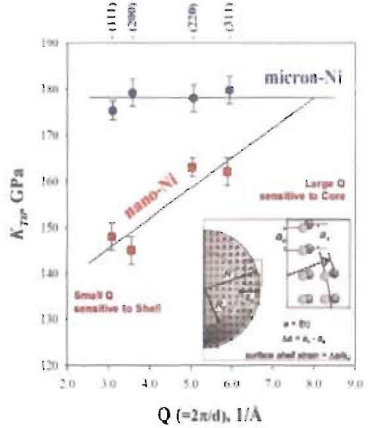

- **Apparent lattice parameters, associated with the specific values of the diffraction *hkl* vectors**
- **Reflections at large Q are associated with the grain core, reflections at small *Q* are sensitive to the surface structure of the nano-grains**

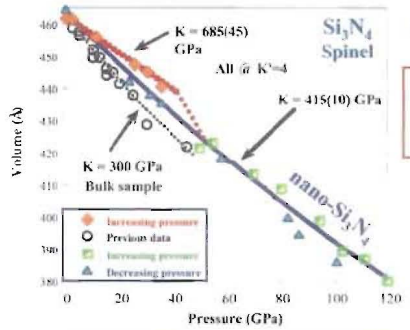

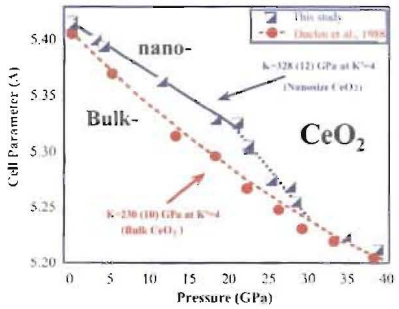

Ge_3N_4 and CeO_2 behave similarly as Si_3N_4

Nanocrystalline ceramics Si_3N_4, Ge_3N_4, and CeO_2 have a ~40 percent higher elastic modulus than their microcrystalline bulks (→ compressed shell)

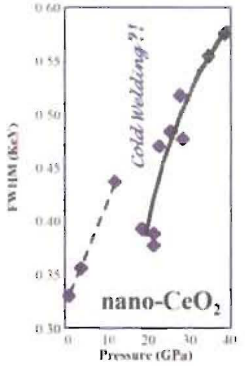

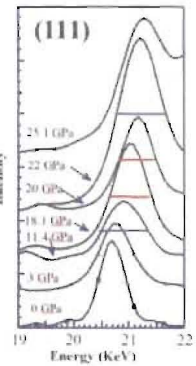

Ceramic nano-CeO_2 with the compressed shell shows work-weakening at transition pressure

Palosz et al., MRS Symp. Proc. (2003)

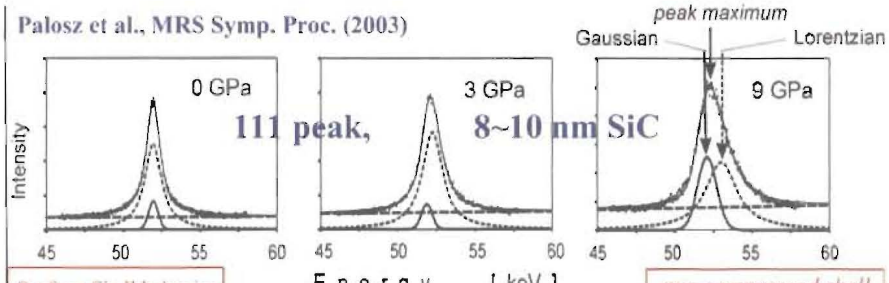

***initial* incompressibility & stress concentration**

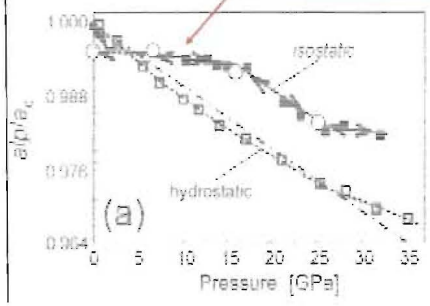

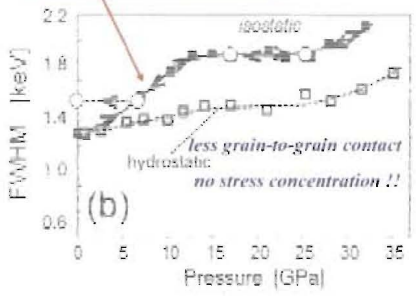

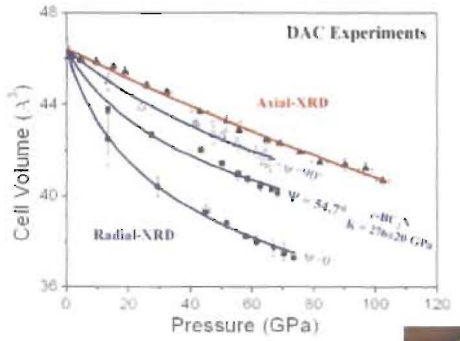

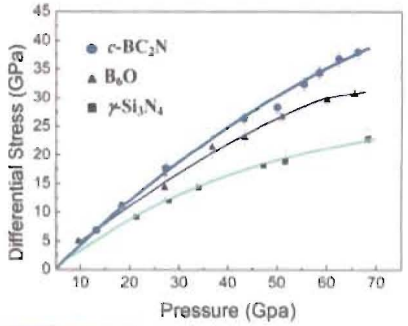

Pressure loading and diffraction reading are very important in data analysis and result derivation. *be very careful* !!!

- **diamond:** K=442 GPa
- **c-BN:** K=367 GPa
- **BC_2N:** K=276 GPa

* Nanocrystals BC_2N embedded in diamond-like amorphous carbon enhance its hardness?!

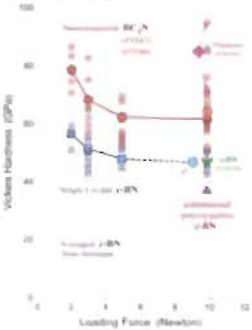

Diamond-SiC composites

synthesis condition: 5 GPa, 1800 K, 30 sec

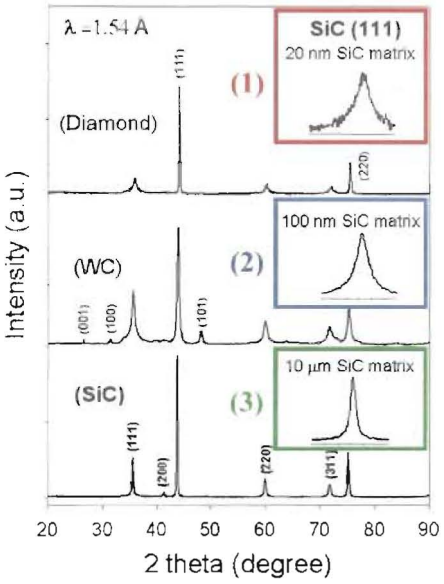

- **Hybrid micron-/nano- diamonds and nano-SiC matrix**
- **High *P-T* reactive sintering removes diamond defects**
- **Reduction of un-reacted silicon and back-transformed graphite**

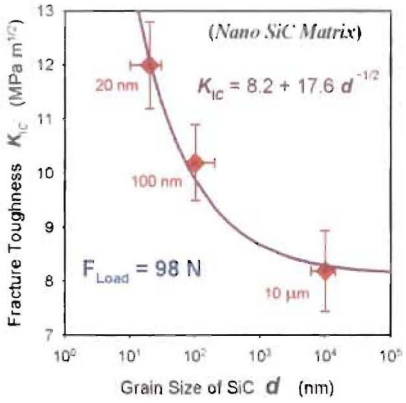

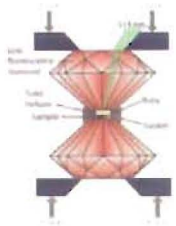

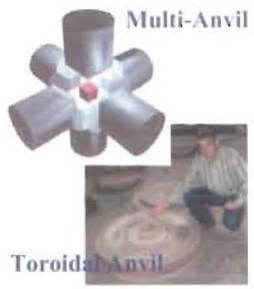

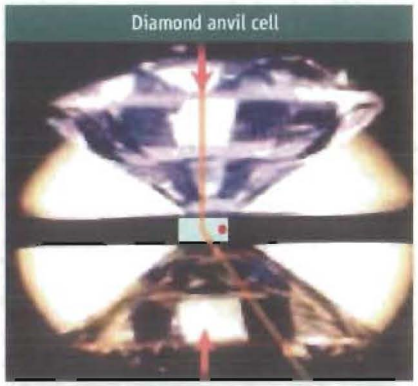

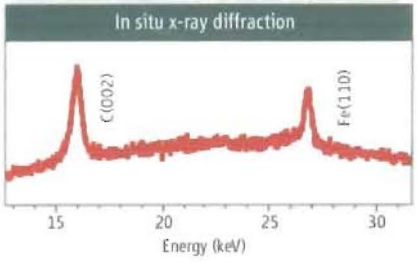

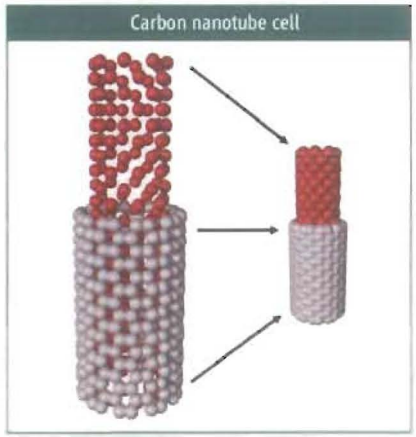

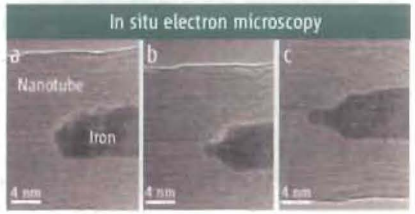

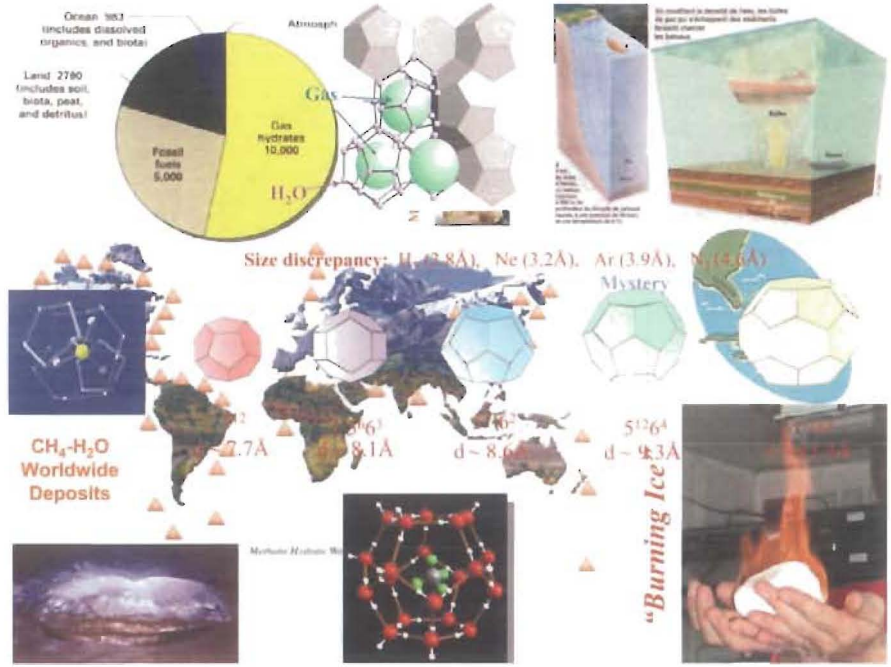

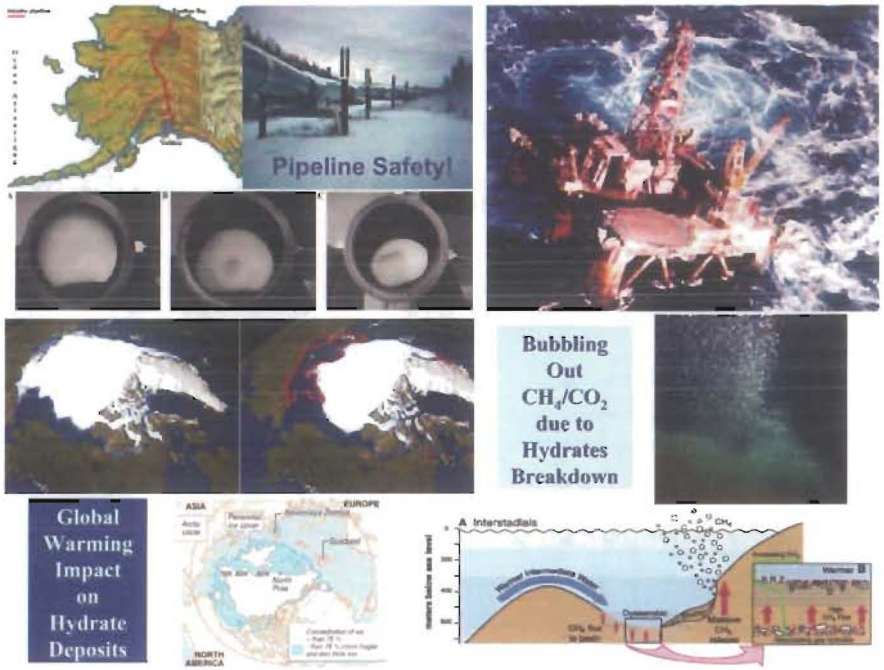
Pipeline Safety!
Bubbling Out CH_4/CO_2 due to Hydrates Breakdown
Global Warming Impact on Hydrate Deposits
ASIA
EUROPE
NORTH AMERICA
A Interstadials

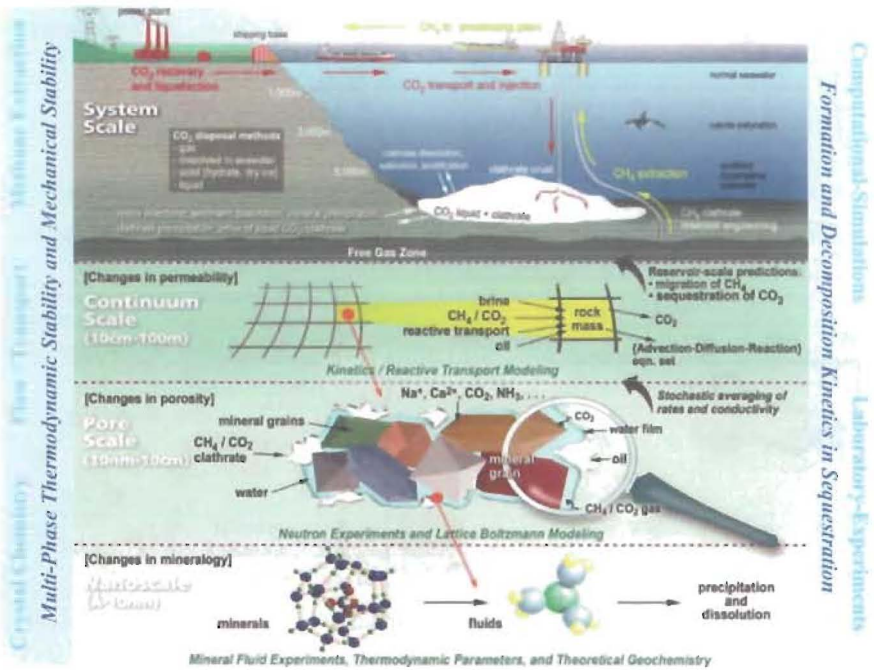
Multi-Phase Thermodynamic Stability and Mechanical Stability
Formation and Decomposition Kinetics in Sequestration
Crystal Chemistry
Flow Transport
Molecular Interaction
Computational Simulations
Laboratory Experiments
System Scale
Free Gas Zone
[Changes in permeability]
Continuum Scale
brine
CH_4 / CO_2 reactive transport
oil
rock mass
CO_2
(Advection-Diffusion-Reaction) eqn. set
Kinetics / Reactive Transport Modeling
[Changes in porosity]
Pore Scale
mineral grains
CH_4 / CO_2 clathrate
water
water film
oil
CH_4 / CO_2 gas
Neutron Experiments and Lattice Boltzmann Modeling
[Changes in mineralogy]
minerals
fluids
precipitation and dissolution
Mineral Fluid Experiments, Thermodynamic Parameters, and Theoretical Geochemistry

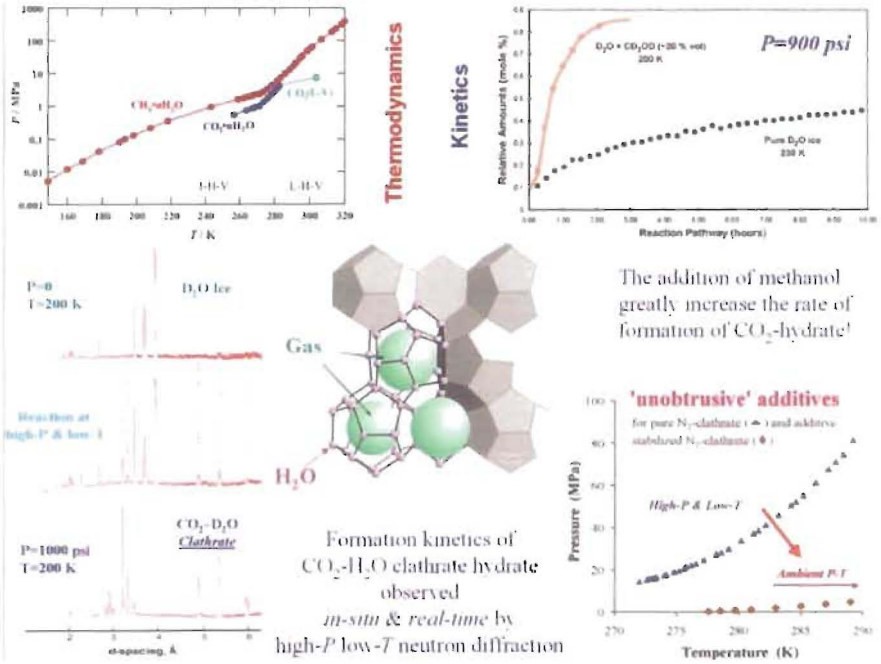
Thermodynamics
Kinetics
CH_4•nH_2O
CO_2•nH_2O
H-H-V
L-H-V
P=900 psi
Pure D_2O ice
Reaction Pathway (hours)
D_2O ice
Gas
H_2O
CO_2-D_2O Clathrate
'unobtrusive' additives
High-P & Low-T
Ambient P, T
Pressure (MPa)
Temperature (K)
The addition of methanol greatly increase the rate of formation of CO_2-hydrate!
Formation kinetics of CO_2-H_2O clathrate hydrate observed *in-situ* & *real-time* by high-*P* low-*T* neutron diffraction

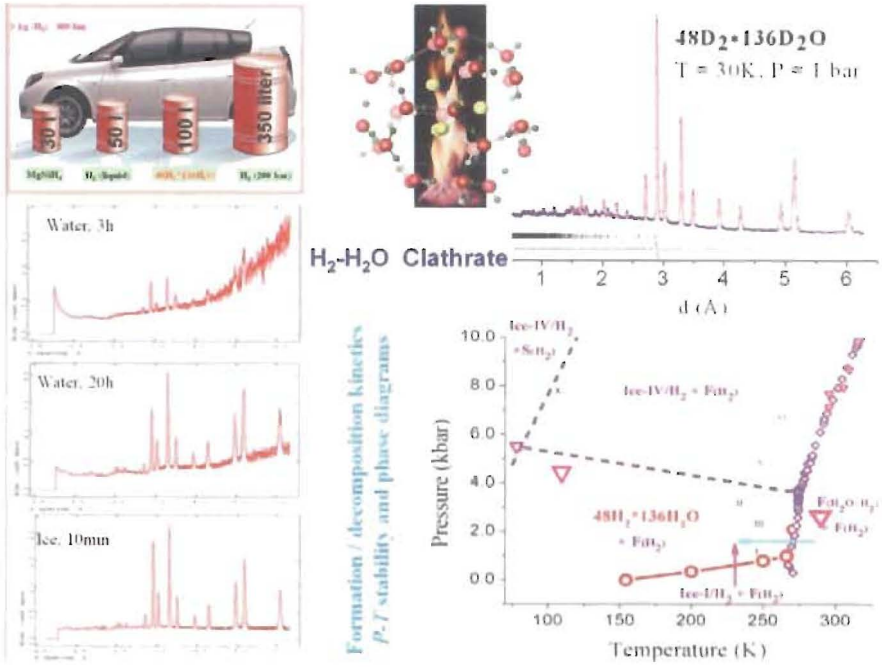
30 l
50 l
100 l
350 liter
Water, 3h
Water, 20h
Ice, 10mn
$48D_2$•$136D_2O$
T = 30K, P = 1 bar
H_2-H_2O Clathrate
d (Å)
Formation / decomposition kinetics
P-T stability and phase diagrams
Ice-IV/H_2 + H_2O
Ice-I/H_2 + FH_2
$48H_2$•$136H_2O$ + FH_2
Pressure (kbar)
Temperature (K)

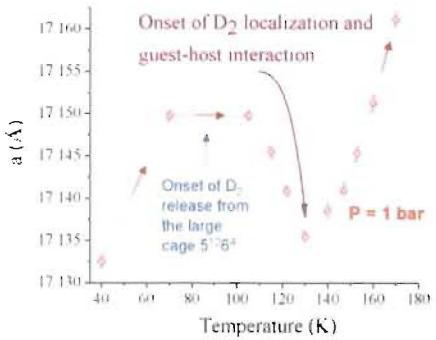

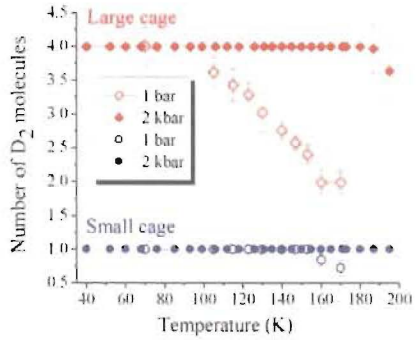

P = 1 bar
T = 50 K

Clathrate Hydrate

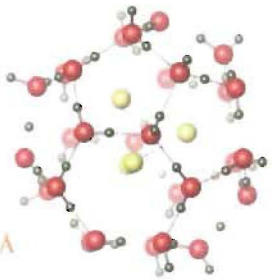

$d_{H2\text{-}H2}$ ~ 2.93 Å

Theory ?

?!

Molecule Model ?

P = 1 bar
T = 14 K

Solid (*hcp*) Hydrogen

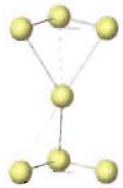

$d_{H2\text{-}H2}$ ~ 3.76 Å

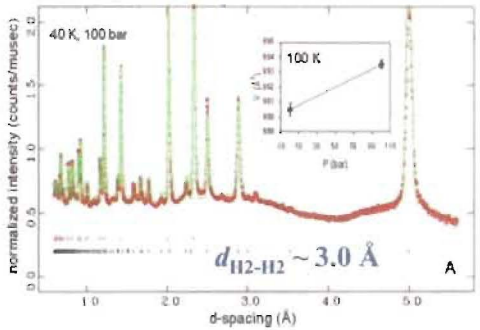

$d_{H2\text{-}H2}$ ~ 3.0 Å

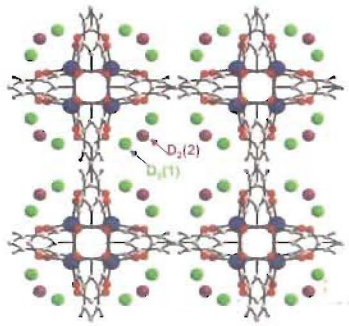

high-*P*/low-*T* neutron diffraction to reveal H_2 adsorption mechanism

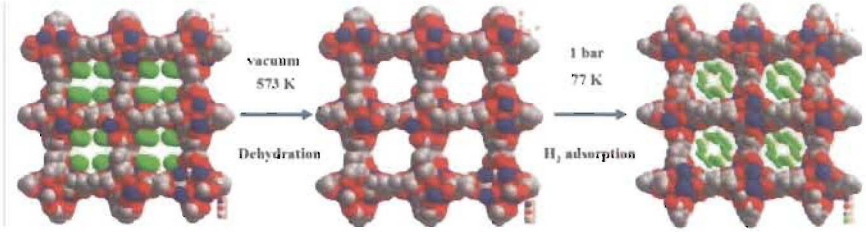

Gas Adsorption

Hydrogen uptake at 77 K

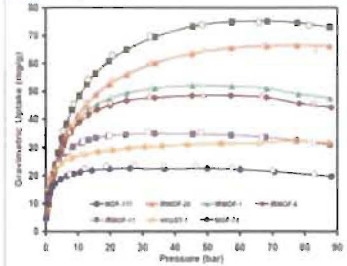

Correlation of uptake with surface area

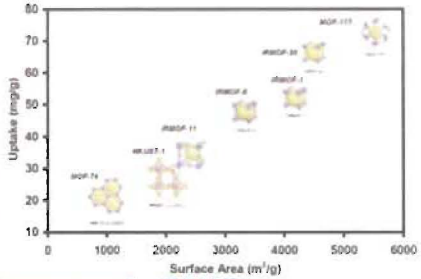

The metal-organic framework (MOF)

Y(BTC)(H2O)·4.3H2O (BTC = 1,3,5-benzenetricarboxylate) for the present case.

MOFs show striking pressurizing effect by the cages. Owing to the enormous variety and flexibility of the frameworks, MOFs may offer superior properties for hydrogen storage.

host-guest interactions (quantum clustering)

Hydrogen Clathrate Hydrate

Cage Structure

$d_{H2\text{-}H2}$ ~ 2.9 Å

20~22% reduction of the bond length in *hydrogen cluster* need to apply as much as 10's kbar in pressure !!!

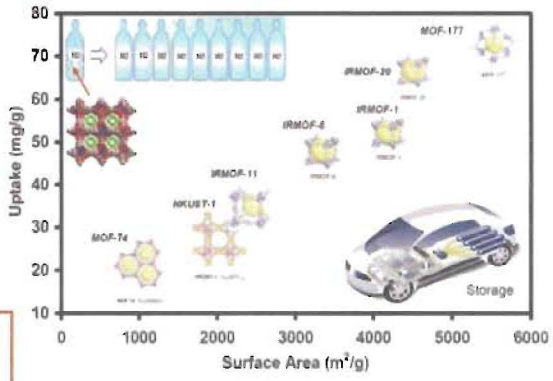

$d_{H2\text{-}H2}$ ~ 3.76 Å

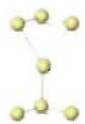

Solid Hydrogen

Metal-Organic Framework

$d_{H2\text{-}H2}$ ~ 3.0 Å

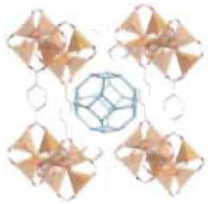

The host nano-encapsulation shows strong *pressurizing* effects applied on the guest

Porous Cage/Channel Structures

Molecular Encapsulation Frameworks